

# LINEAR PREDICTIVE CODING AS A VALID APPROXIMATION OF A MASS SPRING DAMPER MODEL FOR ACUTE STRESS PREDICTION FROM COMPUTER MOUSE MOVEMENT

Lawrence H. Kim<sup>1a</sup>, Rahul Goel<sup>2a</sup>, Jia Liang<sup>3</sup>, Mert Pilanci<sup>4</sup>, Pablo E. Paredes<sup>1</sup>

<sup>1</sup> Department of Psychiatry and Behavioral Sciences, Stanford University, Stanford, CA, USA

<sup>2</sup> Department of Radiology, Stanford University, Stanford, CA, USA

<sup>3</sup> Institute for Computational and Mathematical Engineering, Stanford University, Stanford, CA, USA

<sup>4</sup> Department of Electrical Engineering, Stanford University, Stanford, CA, USA

<sup>a</sup>these authors contributed equally

## ABSTRACT

Prior work demonstrated the potential of using Linear Predictive Coding (LPC) to approximate muscle stiffness and damping from computer mouse (a.k.a. mouse) movement to predict stress levels of users. Theoretically, muscle stiffness in the arm can be estimated using a mass-spring-damper (MSD) biomechanical model of the arm. However, the damping frequency and damping ratio values derived using LPC have not yet been compared with those from the theoretical MSD model. In this work, we demonstrate the damping frequency and damping ratio from LPC are significantly correlated with those from MSD model, thus confirming the validity of using LPC to infer muscle stiffness and damping. We also compare the stress level binary classification performance using the values from LPC and MSD with each other and with neural network-based baselines. We found comparable performance across all conditions demonstrating the efficacy of LPC and MSD model-based stress prediction.

**Index Terms**— Passive Stress Sensing, Linear Predictive Coding, Mass-Spring-Damper Model

## 1. INTRODUCTION

Stress is an instrumental factor for the emotional, cognitive, and physical well-being of people. A large corpus of research has demonstrated strong links between stress and a wide range of chronic health risks such as cardiovascular disease [1], diabetes [2], hypertension [2], obesity [2], and coronary artery disease [3]. Physiological reactions induced by stress are symptomatic of mental illnesses such as anxiety disorder and depression which is a leading cause of suicides [4]. Chronic stress can also lead to mood swings, social isolation, and even reduction in academic achievement among adolescents [5].

Repurposed use of everyday technologies has been proposed to continuously monitor and detect acute stress levels of individuals [6], [7]. Sun et al. demonstrated in the MouStress paper, the effectiveness of using mouse motion data from a computer to measure acute stress where the damped frequency values were larger under a stressed condition than a calm condition [6]. Steering wheels of a car simulator were also successfully used as a sensor for acute stress detection with only a few turns [7].

In both studies mentioned above, the LPC filtering technique was used to infer the fundamental parameters of an MSD system such as the damping frequency and the damping ratio. However, neither study showed if the LPC approach produces values correlated with those from a theoretical MSD model. Thus, in this study, we use the point-and-click dataset from the MouStress study [6] since clicking is the most frequent mouse event accounting for approximately 70% of all events [8], and demonstrate the significant correlation between the damping frequency and damping ratio from a theoretical MSD model and LPC approach. We also compare the stress level binary classification performance using the parameter values from the two approaches (MSD and LPC) with each other and with neural network-based baselines such as CNN and LSTM. Our results demonstrate that LPC and MSD-based stress prediction yields a similar level of accuracy as the neural network-based baselines.

## 2. BIOMECHANICAL MODEL OF THE ARM

### 2.1 Mass-Spring-Damper (MSD) Model

What precedes clicking is a rapid, goal-directed skilled movement. This skilled movement is primarily open-loop in nature, and is influenced by feedforward use of sensory information obtained in previous movements and experience [9]–[13]. The dynamic behavior during any routine skilled movement is influenced by passive joint properties, initial

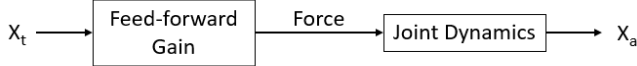


**Fig.1** Open-loop feed-forward model for rapid goal-directed finger movement.

motor commands, sensory feedback, mechanical constraints, and mechanics of the neuromuscular system, aka, biomechanics [14]. Research in the area of biomechanics has shown that a rapid goal directed movement can be modeled as a step response of a linear second order system, i.e., a classic mass-spring damper system [9]–[13]. Typically, smoothed raw movement data is fit to a simple open-loop feedforward model [12], [13].

Fig.1 shows the structure of the model describing the relationship between the target ( $X_t$ ) and the actual ( $X_a$ ) mouse position in the horizontal direction. The open loop transfer function between  $X_t$  and  $X_a$  is given by Eq. 1 as:

$$\frac{X_a(s)}{X_t(s)} = \frac{K_f}{Js^2 + Bs + K} \quad (1)$$

where,  $K_f$  represents the feed-forward gain,  $J$  represents the moment of inertia of the hand,  $B$  is the viscous damping coefficient of the damper and  $K$  is the stiffness of the spring. Eq. 1 can also be represented as:

$$\frac{X_a(s)}{X_t(s)} = \frac{K_p \omega^2}{s^2 + 2\zeta\omega s + \omega^2} \quad (2)$$

where,  $K_p$  is the static gain,  $\omega$  is the un-damped natural frequency, and  $\zeta$  is the damping ratio. Parameters ( $K_p$ ,  $\omega$ ,  $\zeta$ ) were estimated using an iterative time-domain identification technique called prediction-error minimization (“pem” from the System Identification Toolbox of MATLAB) that minimizes the cost function defined as sum of squares of the difference between the actual and the simulated output. Normalized root mean square error was used to estimate the goodness of fit (GOF) of the model and is expressed as:

$$100 \times \left( 1 - \frac{\|X_a - X_s\|}{\|X_a - \text{mean}(X_a)\|} \right) \quad (3)$$

where,  $X_s$  is the simulated step response from the model.

## 2.2 Linear Predictive Coding Filtering Technique

Linear predictive coding (LPC) is a signal filtering technique which builds a predictive model of future samples based only on linear combinations of observed signals from the past [15]. LPC model assumes an all-pole filter that can approximate systems where poles are dominating signal characteristics. It turns out that an ideal second-order system, such as the MSD system described earlier, is an all-pole system in the Laplace domain, and it has a simple second-order LPC model. That is, each sample can be predicted exactly from the previous two, given the MSD parameters. Conversely if we build a second-order LPC model that best fits a series of samples, we can recover the MSD parameters.

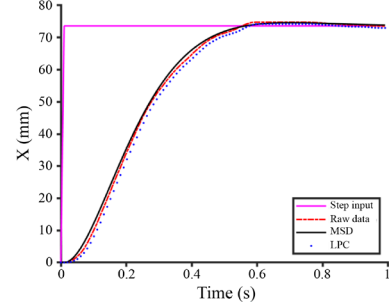


**Fig.2** An example of raw data compared with the responses from MSD and LPC.

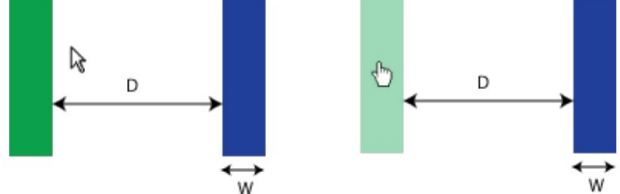


**Fig.3** Point-and-click task from MouStress [6]. Targets are dimmed when clicked- on to provide feedback.

$$H(z) = \frac{1}{A(z)}, A(z) = \frac{E(z)}{X(z)} = 1 - \sum_{k=1}^p a_k z^{-k} \quad (4)$$

where  $H(z)$  is the system response,  $A(z)$  are the LPC coefficients,  $E(z)$  is the system approximation error,  $p$  is the order of the approximation.

As described in the MouStress study [6], LPC is applied to a trajectory with an interpolation order of  $p=4$  as an input. LPC generates a sequence of coefficients that define the characteristic polynomial of the MSD system. This polynomial's complex roots ( $r$ ) characterize the MSD's damping behavior. Specifically, the damping frequency ( $\omega$ ) is the imaginary part of the complex root ( $\omega = |I(r)|$ ), and the damping ratio ( $\zeta$ ) is the ratio of the root's real part and its absolute value ( $\zeta = |R(r)|/|r|$ ).

## 3. METHODOLOGY

Using the dataset from MouStress, we compute the damped frequency,  $\omega$ , and damping ratio,  $\zeta$ , using the MSD model and LPC approach. Fig.2 shows an example of the resulting responses from MSD and LPC compared to the raw signal. Then, we compute the correlation between the  $\omega$  and  $\zeta$  from both methods and compare the classification performance when using LPC and MSD  $\omega$  and  $\zeta$ .

### 3.1. Dataset

We used the mouse motion data from MouStress [6], specifically the *point-and-click* task dataset as clicking is the most frequent mouse event [8]. As the MSD model assumes rapid goal-directed movement, we primarily leverage the mouse movement data that occurs before the click to compute the  $\omega$  and  $\zeta$  using MSD and LPC. As described in the

MouStress paper and shown in Fig. 3, the objective of the user was to move and click the two targets in succession (left and right) as quickly and accurately as possible. Two task parameters, distance D (64px, 128px, 256px, 512px, 1024px) and width W (8px, 16px, 32px, 64px), were varied. Each of the  $N = 49$  participants performed 5 repetitions of the task with the same configuration under both stressed and calm conditions.

### 3.2. Correlation Analysis

To find the correlation between the  $\omega$  and  $\zeta$  from MSD and LPC, we conducted a Spearman's rank correlation for different thresholds of GOF ranging from 0% to 95%.

### 3.3. Stress Classification

We compared four different methods that are based on two decision trees with parameters ( $\omega$  and  $\zeta$ ) derived from MSD and LPC, respectively and two neural network-based (LSTM and CNN) using smoothed raw mouse movement data. Our goal is to compare the MSD and LPC based methods with neural network baselines which do not leverage any domain knowledge or processing. To minimize the effects of personal differences and distance of point-and-click tasks on the performance of the tasks, we decided to build a different classifier per participant per distance of the point-and-click task. This led to each classifier having 40 data samples (20 trials for stressed and 20 trials for calm). Based on the data, we did not see significant influence of the width and thus did not take it into consideration.

For each trial, the dataset consists of the x-position of the mouse at a fixed time interval. As a result, the input of the classifier for LSTM and CNN is a time-series, and the output of the classifier is the stress condition (either stressed or calm). Since the same participant in each trial may finish the point-and-click task at different times, the length of the time-series data as input could be of different length. Thus, we decided to use the LSTM network-based method as our first attempt. However, the direct application of the LSTM model on the raw data turned out not to be successful (manifested by the nondecreasing of the loss function). Further investigation of the raw data revealed that for all trials, the final value of x position of each time series was generally repeated for many times. As a result, the last several points in each time-series looked very similar regardless of the stress condition. Thus, we let the LSTM network learn from windowed time-series data with the ending parts removed. To implement this, we fixed a cutoff value (representing the last points of the new time-series) for all the point-and-click tasks of the same distances. The cutoff values were set to be 100 ms for 64x, 125 ms for 128x, 150 ms for 256x, 350 ms for 512x, and 500 ms for 1024x. To make a fair comparison, the same cutoff values applied to inputs of LSTM models were also applied to that of CNN models.

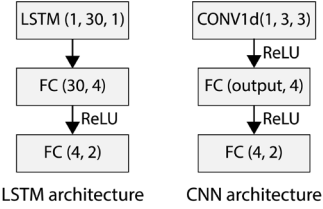


**Fig.4** Architecture of the methods based on LSTM and CNN. (FC = fully connected layer, ReLU = rectified linear unit)

Due to the scarcity of our data, the final version of the LSTM model used only consisted of one LSTM layer followed by two fully-connected layers, and its architecture is shown in Fig. 4. The LSTM based model was trained with Stochastic Gradient Descent Optimizer with cross-entropy loss as the loss function. The batch size was equal to 4, and the learning rate was fixed at 0.05. We split our data into the training set, validation set, and test data with the following ratio: 60%, 20%, 20%; moreover, in training, validation, and test datasets, we enforced the condition that the number of trials performed under the stressed condition is equal to that under the calm condition. The model was trained from scratch for 100 epochs, and the model with the best validation accuracy during the training was saved and used to infer the test accuracy.

The final architecture of the CNN model is shown in Fig. 4. The CNN model was trained exactly like the LSTM based model as described above with a learning rate of 0.001, and the model was trained for 500 epochs. All the neural network models were implemented using Pytorch.

For the MSD-based classifier, we extracted a pair of  $\omega$  and  $\zeta$  values from the full segments of each time series. Then, this paired value was then fit with the decision tree classifier with default hyperparameters imported from the *sklearn* library. The accuracy was obtained from averaging accuracies from the 5-fold cross-validation. The LPC-based classifier was trained and evaluated in the same way using  $\omega$  and  $\zeta$  values derived from the LPC filter. The overall process (extraction of damping frequency features, fitting decision tree, obtaining classification accuracy) described above was repeated 100 times for both MSD and LPC based methods, and the average results are reported in Table 1.

## 4. RESULTS & DISCUSSION

Fig. 5 shows examples of all the mouse motion trajectories from a participant under stressed and calm conditions before applying the cutoff. Fig. 5a demonstrates mouse trajectories with clear distinction between the stressed and calm conditions. Such trends were noticed visually for 32 of the 49 participants. Fig. 5b shows a case where no clear boundary could be drawn between the trajectories under stressed and calm conditions. 17 participants visually exhibited similar behavior.

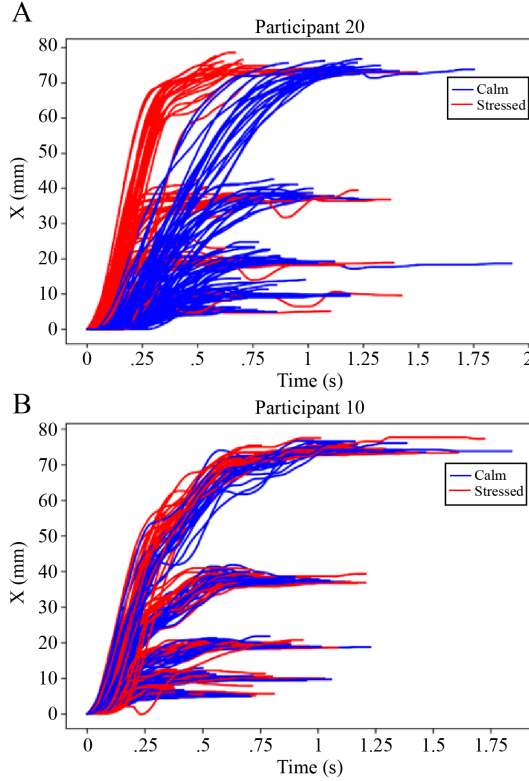


**Fig.5** An example of mouse pointer trajectories from a participant a) with, b) without clear boundaries between the *stressed* (Red) and *calm* (Blue) conditions.

#### 4.1. Correlation

Fig. 6 shows the results for correlations between the damping frequencies and damping ratios from MSD and LPC for different thresholds of GOF. All correlations were statistically significant ( $p < 0.001$ ). The correlation coefficient between the damping frequencies reached 0.7 and went even higher for data with GOF of at least 80%. For the correlation coefficient between the damping ratios, we saw milder correlation of approximately -0.45 even for data with GOF of 90%. As the threshold for GOF reached 80%, we saw a steeper decline in percentage of data that met the requirement as shown in Fig. 6, where only around 55% of the data met the 80% GOF threshold criteria, typically used in system modeling studies.

#### 4.2. Stress Binary Classification Accuracy

Table 1. shows the classification accuracies from the four methods. The MSD-based model had the highest overall accuracy followed by LPC, LSTM and CNN-based models. This result suggests that the simple MSD and LPC models have the potential to match or outperform neural network-based models for predicting acute stress levels. In the future, it may be worth exploring whether using only the data samples above certain GOF or error variance improves the accuracies of the MSD and LPC based classifiers.

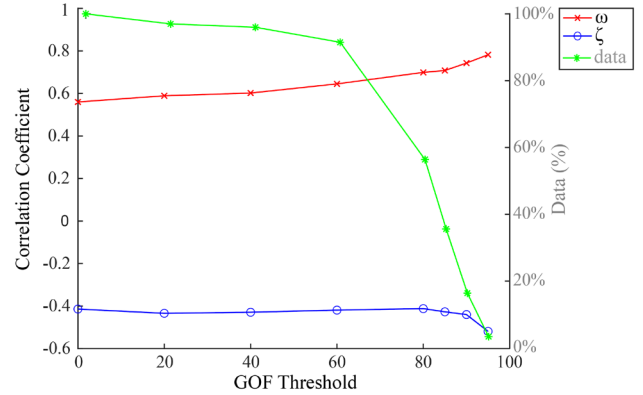


**Fig.5** The correlation coefficients between the  $\omega$  and  $\zeta$  from MSD and LPC for different thresholds of GOF are shown with red and blue lines, respectively. The green line indicates the percentage of the corresponding data according to different thresholds of GOF.

**Table 1.** Comparison of stress level binary classification accuracy across the four approaches. Note that for both MSD and LPC, the accuracies were the average results of 100 different trials.

Distance	CNN	LSTM	MSD	LPC
64x	53.57%	53.83%	58.07%	55.74%
128x	54.34%	53.06%	58.47%	57.21%
256x	54.59%	59.18%	60.79%	59.33%
512x	59.95%	66.58%	64.82%	62.99%
1024x	62.76%	68.11%	70.18%	67.93%
Overall	<b>57.04%</b>	<b>60.15%</b>	<b>62.47%</b>	<b>60.64%</b>

It is also worth noting the reduction in accuracy observed with smaller distances between targets. A possible explanation for this reduction is that as the targets are closer together, there is less interaction from the larger muscles in the arm versus the hand. Another possibility is that the truncation window used for the different classifiers could play a role. As we progress towards “in the wild” studies, it would be relevant to study finding the optimal “window” length to apply MSD or LPC-based estimators.

## 5. CONCLUSION

In this paper, we demonstrate the use of the LPC technique as an approximation to a biomechanical MSD model of the human arm to predict acute stress levels of users based on their computer mouse movement data. We also compared their stress classification performance to that of neural network-based models such as LSTM and CNN and found that MSD and LPC-based models produced higher classification accuracies than LSTM and CNN-based models. This demonstrates the potential of LPC and MSD models in predicting the stress levels of users from their mouse movement data. In the future, we plan to explore using a combination of neural network-based approaches with MSD or LPC and applying those methods to analyze in-the-wild data.

## 12. REFERENCES

- [1] P. L. Schnall, P. a Landsbergis, and D. Baker, "Job Strain and CARDIOVASCULAR DISEASE Peter," *Annu. Rev. Public Health*, no. 9, pp. 381–411, 1994.
- [2] D. N. Brindley and Y. Rolland, "Possible Connections between Stress, Diabetes, Obesity, Hypertension and Altered Lipoprotein Metabolism that may Result in Atherosclerosis," *Clinical Science*, vol. 77, no. 5, pp. 453–461, Nov. 1989.
- [3] T. G. Pickering, "Mental stress as a causal factor in the development of hypertension and cardiovascular disease," *Current Hypertension Reports*, vol. 3, no. 3, pp. 249–254, 2001.
- [4] G. M. Slavich and R. P. Auerbach, "Stress and its sequelae: Depression, suicide, inflammation, and physical illness," *APA handbook of psychopathology: Psychopathology: Understanding, assessing, and treating adult mental disorders (Vol. 1)*, vol. 1, pp. 375–402, 2018.
- [5] K. Schraml, A. Perski, G. Grossi, and I. Makower, "Chronic Stress and Its Consequences on Subsequent Academic Achievement among Adolescents," *Journal of Educational and Developmental Psychology*, vol. 2, no. 1, pp. 69–79, 2012.
- [6] D. Sun, P. Paredes, and J. Canny, "MouStress: Detecting stress from mouse motion," *Conference on Human Factors in Computing Systems - Proceedings*, pp. 61–70, 2014.
- [7] P. E. Paredes, F. Ordoñez, W. Ju, and J. A. Landay, "Fast & furious: Detecting Stress with a car steering wheel," *Conference on Human Factors in Computing Systems - Proceedings*, vol. 2018-April, pp. 1–12, 2018.
- [8] M. Antal and E. Egyed-Zsigmond, "Intrusion detection using mouse dynamics," *IET Biometrics*, vol. 8, no. 5, pp. 285–294, 2019.
- [9] J. Müller, A. Oulasvirta, and R. Murray-Smith, "Control theoretic models of pointing," *ACM Transactions on Computer-Human Interaction*, vol. 24, no. 4, 2017.
- [10] F. Fischer, A. Fleig, M. Klar, L. Gruene, and J. Mueller, "An Optimal Control Model of Mouse Pointing Using the LQR," 2020, [Online]. Available: <http://arxiv.org/abs/2002.11596>.
- [11] S. Aranovskiy, R. Ushirobira, D. Efimov, and G. Casiez, "A switched dynamic model for pointing tasks with a computer mouse," *Asian Journal of Control*, vol. 22, no. 4, pp. 1387–1400, 2020.
- [12] R. Goel and W. H. Paloski, "Motor Control Performance During Rapid Voluntary Movements of Elbow and Knee," *Journal of Motor Behavior*, vol. 48, no. 4, pp. 348–356, 2016.
- [13] L. B. Bagesteiro and R. L. Sainburg, "Nondominant arm advantages in load compensation during rapid elbow joint movements," *Journal of Neurophysiology*, vol. 90, no. 3, pp. 1503–1513, 2003.
- [14] F. Popescu, J. M. Hidler, and W. Z. Rymer, "Elbow impedance during goal-directed movements," *Experimental Brain Research*, vol. 152, no. 1, pp. 17–28, 2003.
- [15] D. O. Shaughnessy, "Linear predictive coding," *IEEE Potentials*, vol. 7, no. 1, pp. 29–32, 1988.